EFDA–JET–CP(14)01/09

D. Tskhakaya, M. Groth and JET EFDA contributors

Modelling of Tungsten Re-Deposition Coefficient

Modelling of Tungsten Re-Deposition Coefficient

D. Tskhakaya[1,3], M. Groth[2] and JET EFDA contributors*

JET-EFDA, Culham Science Centre, OX14 3DB, Abingdon, UK

[1]Association EURATOM-ÖAW, Institute of Applied Physics, TU Wien, A-1040 Vienna, Austria
[2]Aalto University, Association EURATOM-Tekes, Otakaari 4, 02015 Espoo, Finland
[3]Permanent address: Andronikashvili Institute of Physics, 0177 Tbilisi, Georgia
** See annex of F. Romanelli et al, "Overview of JET Results",*
(24th IAEA Fusion Energy Conference, San Diego, USA (2012)).

Preprint of Paper to be submitted for publication in Proceedings of the
21st International Conference on Plasma Surface Interactions, Kanazawa, Japan
26th May 2014 – 30th May 2014

ABSTRACT

We study tungsten prompt re-deposition process at the divertor plates via kinetic modelling of the JET SOL for different divertor plasma parameters. Our simulations demonstrate that contrary to the present assumptions the electric field and not the Lorentz Force is the major contributor to the prompt re-deposition process. The fraction of tungsten ions escaping from the divertor plasma is defined by the number of tungsten atoms ionized outside the magnetic sheath and does not exceed 3% of the ion sputtered from the divertor surface. We derived the corresponding fit function for estimation of the re-deposition coefficient.

1. INTRODUCTION

Tungsten is a favorable divertor surface material in present-day and future tokamaks [1]. However, tungsten sputtering and penetration into the core can lead to significant radiation reducing plasma performance. As a result, the development of precise models of tungsten generation and transport in the plasma edge is one of critical tasks in fusion plasma study. Among others, the effective tungsten sputtering yields is of particular interest. Due to low ionization potential W atoms can be ionized in the vicinity of the divertor and re-deposit back to the divertors without contribution to the actual sputtering [2 - 6]. Therefore, it is necessary to estimate the effective tungsten sputtering yields, or re-deposition coefficient, f_{prompt}: $Y_{eff} = (1 - f_{prompt})Y$. Commonly accepted model of this re-deposition (or so called *prompt* re-deposition) is based on the assumption that ions ionized near the divertor plates re-deposit due to Larmor rotation. By assuming that all W atoms are ionized at the distance l_{ion} from the divertors surface and neglecting all other forces except the Lorentz force one obtains the following analytic expression [4, 6]:

$$f_{prompt}\,(n_e\,,\,T_e) = \left(1 + (l_{ion} / \rho_W)^2\right)^{-1}, \qquad (1)$$

where n_e , T_e , B and ρ_W are the electron density and temperature, the strength of the magnetic field and the Larmor radius of the (singly ionized) W ion.

In reality, there are other forces acting on W ions, which (as we see below) can not be in general neglected in estimation of f_{prompt} [7, 8]. The forces acting on W ions near the divertor plates are: the force of sheath electric field $F_E = Z_w e E_n$; The Lorentz force $F_L = Z_w e[V_W \times B]_n$; the main ion drag, $F_d \approx m_w V_{i,n} \nu_{sd}$, and the thermal, $F^i_{th} \approx \alpha_i Z_w^2 \partial T_i / \partial x$, forces; as well as the electron thermal force $F^e_{th} \approx \alpha_e Z_w^2 \partial T_e / \partial x$. Here, m_w, V_W, V_i and $T_{e,i}$ denote the W ion mass and velocity, the main ion flow velocity, and the electron and the main ion temperatures; furthermore, the subscript "n" denotes a projection to the normal to divertor surface directed along the x axes, ν_{sd} is the slowing-down collision frequency [9], and $\alpha_{e,i}$ coefficients of the order of unity [10, 11]. We note that the plasma sheath, where the re-deposition process takes the place, is a strongly non-uniform layer where ions are not fully magnetised. Hence, the above-given expressions for F_d and $F^{e,i}_{th}$ are used just for quantitative estimation of the corresponding forces.

The aim of the present work is to investigate tungsten re-deposition process via kinetic modelling, where all forces acting on W ions are included in a self-consistent manner.

2. DESCRIPTION OF THE SOL MODEL

The forces acting on W as well as plasma parameters in front of divertor plates can strongly depend on the velocity distribution functions (VDF) of the electrons the main ions in the plasma boundary [12]. In order to self-consistently obtain particle VDF in the divertor plasma we consider a slab model of the SOL bounded between the two divertor plates, separatrix and outer wall. This model is simulated by quazi-2D electro-static massively parallel PIC/MC (Particle in Cell/Monte Carlo) code BIT1 [7, 13].

The code simulates the electrons, the main ions (D+), the neutrals (D, C, W) and the impurity ions (W^{n+}, C^{m+}, n = 1,..,6, m = 1, 2) taking into account Coulomb and atomic collisions between these particle species. During the simulation hot electrons and D^+ ions with the Maxwelian VDF are injected into the source region, corresponding to the particle and heat transport across the separatrix. D^+ ions (and D atoms) absorbing at the divertor plates are recycled as D atoms with a specified recycling coefficient R. C atoms are injected from the divertor plates at fixed injection rate, $10^{21} m^{-2} s^{-1}$. The C^{m+} impurity is used to cool down electrons at the divertor region to realistic temperatures; the cooling rate is "controlled" by switching on/off the electron – C^{++} excitation collisions.

Neutral particles (treated in 2D approximation) can propagate along the poloidal direction too and are removed from the simulation if they reach the separatrix, or the outer wall. Impurity ions are treated in "quasi-2D": they are removed from the simulation with the "frequency" corresponding to the cross-field diffusion coefficient $D_\perp \sim 1 m^2/s$ and the cross-field gradient length $\sim 1 cm$.

Different SOL parameters, corresponding to the L- and H-mode plasmas, and ELMy SOL, are obtained by changing the following input parameters: i. strengths of the particle (S_p) and the heat (S_h) sources, ii. temperatures of the source particles ($T^0_{e,i}$) iii. The recycling coefficient R, and iv. the electron – C^{++} collisionality. Other details of the simulation model can be found in [7, 14].

Contrary to our previous model (see [7]), in the present work we do not consider complex W sputtering process, but inject Maxwell distributed W atoms at the divertor plates with a given injection rate, $F_W^{inj} = 5 \times 10^{21} m^{-2} s^{-1}$. This value exceeds by the factor ~ 5-8 the sputtered W atom flux density observed in our previous work [7] and chosen as a compromise between the simulation accuracy (increases with increasing flux) and an artificially high concentration of W ions, which is still low enough not to influence significantly divertor plasma parameters. In order to study the dependence of f_{prompt} on the VDF of injected atoms we consider different temperatures of the injected W atoms, T_W^{inj} , from 1 to $15 eV$. This choice of the injection VDF and of the temperature range has been made in order to keep universality, i.e. independence from the sputtering model, and to cover all energies of interest. As an example in Figure 1 are plotted sputtered W atom effective temperatures, $T_W = 2/3 \int E f_{Th}(E) dE$ as a function of impinging particle energy, E_0 , where $f_{Th}(E)$ is a Thompson distribution frequently used in W sputtering models [15]:

$$f_{Th}(E) \sim \frac{E}{(E+E_s)^3}, \quad 0 \le E \le E_{\max} = \frac{4m_0 m_w}{(m_0+m_w)^2} E_0 . \tag{2}$$

Here m_0 and E_s are the impinging particle mass and the corresponding surface binding energy.

The re-deposition coefficient is obtained as $f_{prompt} = F_W^{div}/F_W^{inj}$, where F_W^{div} is a total flux of W ions re-deposited back at the divertor surface.

The set of parameters used in the simulation is given in the table 1. The magnetic field has been assumed to be $2T$. Each case consisted of two sets of simulation: first, the stationary state has been reached without W injection; then W atoms have been injected from the divertors until a new stationary state has been reached (after few W^+ gyro-periods, τ_W). All the results have been averaged over τ_W. In the simulation we used 60 000 cells along the poloidal direction. The number of the main ions per cell was 45 – 750. Simulations have been performed on 128 – 4096 processors. The CPU time used per case was 50 000 – 250 000 processor hours (strongly depends on SOL parameters).

3. SIMULATION RESULTS

Divertor plasma parameters and the corresponding profiles are given in Table 2 and plotted in Figure 2. These simulations cover wide range of parameters corresponding different discharges at JET. In order to estimate W ion concentration we plotted the profile of $Z_{eff}^W = \sum_i Z_i^2 n_w^i / n_e$, where n_w^i is the density of W^{i+} ions. As we can see the profile of Z_{eff}^W in the divertor plasma depends strongly on the initial energy of W atoms (i.e. T_w), but outside $1cm$ from the divertor surface it drops for any values of T_w. The obtained re-deposition coefficients are plotted in Figure 3, where for convenience we consider $f = 1 - f_{prompt}$. As we can see, the analytic expression (1) underestimates f_{prompt}. The distribution of re-deposited ionization states is plotted in Figure 4. This distribution depends on divertor plasma parameters as well as on the initial energy of W atoms. The later is expected, because energetic W atoms can penetrate deeper into the plasma and after ionization the newly born ions have to travel longer path before they re-deposit to the divertor surface. In general, at least 80% of the re-deposited ion flux is curried by singly and doubly ionized W ions.

In order to understand these results we analyse the forces acting on W ions plotted in Figure 5. As one can see, practically in all the region where most of the W are ionized, x $\in [0, l_{ion}]$, the electric field force by order(s) of magnitude stronger than other forces. Hence, most of the ions re-deposit back due to the sheath electric field and only the ions born outside the strong electric field region (i.e. outside the magnetic sheath) can escape from the divertor plasma. The forces, which can contribute to pulling out of W ions, are the Lorentz and the ion thermal one (other forces are negligibly small). In order to estimate which of these two forces is dominant we print in the table 2 the ratios of the Lorentz and the ion thermal forces to the electric field force at the distance l_{ion} from the divertor surface, $F_L/F_E\big|_{x=l_{ion}}$, $F_{th}^i/F_E\big|_{x=l_{ion}}$. According to these estimates, there is no correlation between $F_L/F_E\big|_{x=l_{ion}}$ and the re-deposition coefficient, while there is a significant correlation between $F_{th}^i/F_E\big|_{x=l_{ion}}$ and f_{prompt}. This indicates that probably the ion thermal force is a main contributor to pulling out of ions from the vicinity of the magnetic sheath.

Let us construct a fit function, which can be used for estimation of f_{prompt}. According to our simulations there are two main parameters defining prompt re-deposition. The first one is related to the number of ions which can born outside is the magnetic sheath and can be characterised by the ratio of W atom ionization length, l_{ion}, to the magnetic sheath width, $\sim \rho_i$ (ρ_i is the main ion gyro-radius). The second parameter is the ratio of the ion thermal force (which is pulling out W ions) to the average electric field (a force pushing back the W ions). In the vicinity of the magnetic sheath we estimate these forces as follows: $F_{th}^i \sim \partial T_i / \partial \mathrm{x} \sim T_i / \rho_i$, $F_E \sim e \partial \Delta\varphi_{sh} / \partial x \sim T_e / \rho_i$, where $\Delta\varphi_{sh} \sim T_e / e$ is the potential drop across the magnetic sheath. Using these parameters we construct a following simple fit function satisfying correct limits, $\lim_{l_{ion}\to\infty} f_{prompt} = 0$, $\lim_{l_{ion}\to\infty} f_{prompt} = 1$:

$$f_{prompt} \approx \left(1 + \alpha \frac{l_{ion}}{\rho_i} \frac{T_i}{T_e}\right)^{-1}, \tag{3}$$

where α is some constant and plasma parameters are taken at the magnetic sheath entrance. In Figure 6 are plotted f_{prompt} from PIC simulation and from the Eq. (3) with $\alpha = 0.01$, showing fairly good agreement.

4. CONCLUSIONS

Prompt re-deposition is a complex process involving the electric field, the Lorentz and the ion thermal forces. Contrary to existing opinion, not the Lorentz, but the electric field is the main contributor to the W ion prompt re-deposition to the divertor plates. Moreover, it seems that the ion thermal force is responsible for the fraction of ions escaping the divertor plasma. For the JET relevant parameters the vast majority of sputtered W is re-deposited back and can't enter the plasma. The fraction of W ions leaving the divertor plasma does not exceed 3% of the sputtered atoms even for most favourable conditions. This fraction can be estimated from the Eq. (3).

In order to apply these results to other machines two conditions have to be satisfied. First, the sheath electric force has to be stronger than the Lorentz force acting on W ions. In other words $F_L / F_E \sim V_W \, eB\rho_i / T_e \sim \sqrt{m_i / m_W} \;\; \sqrt{T_W / T_i} / T_e < 1$. This condition, due to large mass ratio m_W / m_i, is satisfied for most of the divertor plasmas. Second, the majority of W atoms have to be ionized inside the magnetic sheath, $l_{ion} \lesssim 5\rho_i$ (~ typical width of the magnetic sheath). As an example, in Figure 7 is plotted $l_{ion} / 5\rho_i$ as a function of plasma density and temperature for ITER. The dashed line indicates the applicability limit of our model.

ACKNOWLEDGEMENTS.

This work was supported by EURATOM and carried out within the framework of the European Fusion Development Agreement. The views and opinions expressed herein do not necessarily reflect those of the European Commission. Most of the simulations were carried out using the HELIOS supercomputer system at Computational Simulation Centre of International Fusion Energy Research Centre (IFERC-CSC), Aomori, Japan, under the Broader Approach collaboration between Euratom

and Japan, implemented by Fusion for Energy and JAEA. Part of simulations has been performed on Curie (France) and Leo III (Austria) supercomputers. We thank A. Kirschner and S. Brezinsek for useful discussions. The first author acknowledges support by the projects FWF P26544-N27 and WP-PFC PFC.SP4.1.

REFERENCES

[1]. G.F. Matthews, JET EFDA Contributors, the ASDEX-Upgrade Team, Journal of Nuclear Materials, **438** (2013) S2-S10;

[2]. G. Fussmann, W. Engelhardt, D. Naujoks, et al., Plasma Physics, Plasma Physics and Controlled Nuclear Fusion Research, **2** (1994) 143-148;

[3]. D. Naujoks, K. Asmussen, M. Bessendort-Weberpals, et al., Nuclear Fusion, **36** (1996) 671–687;

[4]. R. Dux, A. Janzer, T. Pütterich and ASDEX Upgrade Team, Nuclear Fusion, **51** (2011) 053002;

[5]. S. Brezinsek, D. Borodin, J.W Coenen, D. Kondratjew, M. Laengner, A. Pospieszczyk, U. Samm and the TEXTOR team, Physica Scripta, **T145** (2011) 014016;

[6]. G.J. van Rooij, J.W. Coenen, L. Aho-Mantila, et al., Journal of Nuclear Materials, **438** (2013) S42–S47;

[7]. D. Tskhakaya, M. Groth, JET EFDA contributors, Journal of Nuclear Materials, **438** (2013) S522–S525;

[8]. P.C. Stangeby, D.L. Rudakov, W.R. Wampler, Journal of Nuclear Materials, **438** (2013) S309–S312;

[9]. B.A. Trubnikov, Reviews of Plasma Physics, **1** (1965) 105–204;

[10]. P.H. Rutherford, Physics of Fluids, **17** (1974) 1782–1784;

[11]. D. Reiser, D. Reiter, M.Z. Tokar, Nuclear Fusion, **38** (1998) 165–177;

[12]. D. Tskhakaya, Cont. Plasma Physics, **52** (2012) 490–499 ;

[13]. D. Tskhakaya, A. Sobba, et. al., proceedings of 18-th Euromicro Conference on Parallel, Distributed and Network-based Processing, Pisa Italy, IEEE, 2010, pp. 476–481;

[14]. D. Tskhakaya, S. Jachmich, Th. Eich, et al., Journal of Nuclear Materials, **415** (1), (2011) S860–S864;

[15]. W. Eckstein, IPP report, IPP 9/132, (2002).

Case	S_p m^{-3}s^{-1}	S_h MWm^{-3}	T_p^0 eV	T_i^0 eV	T_W^{inj} eV	e + C^{++}	R
1	2.55 x 10^{22}	1.06	120	250	8.0	off	0.0
2	1.27 x 10^{22}	1.42	120	250	8.0	off	0.95
3	2.55 x 10^{22}	4.47	120	250	8.0	off	0.99
4	2.55 x 10^{22}	4.16	120	250	8.0	on	0.99
5	1.27 x 10^{22}	0.0	700	1200	8.0	off	0.0
6	2.55 x 10^{22}	4.49	120	250	1.0	off	0.99
7	2.55 x 10^{22}	4.47	120	250	5.0	off	0.99
8	2.55 x 10^{22}	4.48	120	250	15.0	off	0.99
9	2.55 x 10^{22}	4.38	120	250	5.0	on	0.99

Table 1: Simulation parameters. The case 5 corresponds to a middle size (~ 300kJ) ELM.

Case		n_e m^{-3}	T_e eV	T_i eV	l_{ion} mm	F_L/F_E	F_{th}^i/F_E	f_{prompt}
1	ID	2.47 x 10^{18}	66.6	47.6	1.89	0.296	1.017	0.9735
	OD	2.37 x 10^{18}	74.1	51.0	1.93	0.278	1.127	0.9777
2	ID	3.82 x 10^{18}	59.9	18.1	1.36	0.153	0.115	0.9933
	OD	3.35 x 10^{18}	69.4	20.1	1.50	0.150	0.139	0.9850
3	ID	3.56 x 10^{19}	25.1	7.6	0.183	0.0501	0.0078	0.9946
	OD	1.94 x 10^{19}	43.0	10.6	0.270	0.0428	0.0041	0.9937
4	ID	7.01 x 10^{19}	8.8	5.3	0.094	0.0720	0.0256	0.9983
	OD	3.25 x 10^{19}	18.9	7.5	0.176	0.0532	0.0154	0.9957
5	ID	3.38 x 10^{18}	199	262	1.12	0.0696	1.184	0.9845
	OD	3.49 x 10^{18}	200	277	1.08	0.0681	1.341	0.9877
6	ID	3.94 x 10^{19}	24.0	7.0	0.169	0.0183	0.0085	0.9968
	OD	1.80 x 10^{19}	44.6	10.9	0.278	0.0163	0.0053	0.9968
7	ID	3.60 x 10^{19}	24.9	7.4	0.181	0.0406	0.0079	0.9976
	OD	1.92 x 10^{19}	43.2	10.5	0.270	0.0342	0.0044	0.9946
8	ID	3.57 x 10^{19}	25.4	7.5	0.183	0.0677	0.0073	0.9995
	OD	1.83 x 10^{19}	44.2	10.6	0.284	0.0586	0.0045	0.9972
9	ID	7.47 x 10^{19}	8.6	5.6	0.086	0.0726	0.0266	0.9991
	OD	3.59 x 10^{19}	18.4	7.6	0.169	0.0535	0.0154	0.9978

Table 2: Divertor plasma parameters from the PIC simulation. All parameters are averaged over 1mm distance from the divertort surface (approximately equals to the width of magnetic sheath). Accuracy of f_{prompt} calculation is 2×10^{-4}. Here and below "ID" and "OD" denote inner and outer divertors, respectively. F_L / F_E and F_{th}^i F_E are force ratios at the distance lion from the divertor surface.

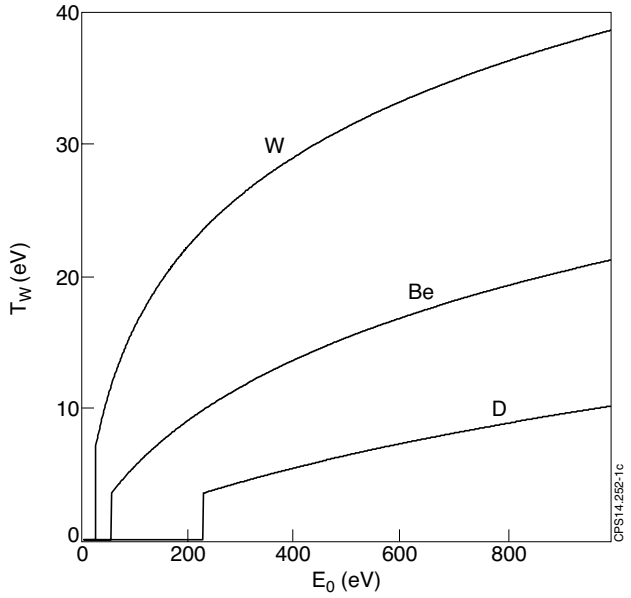

Figure 1: Effective temperature of sputtered W atoms, with Thompson energy distribution (2), as a function of impinging ion (D, Be, W) energy.

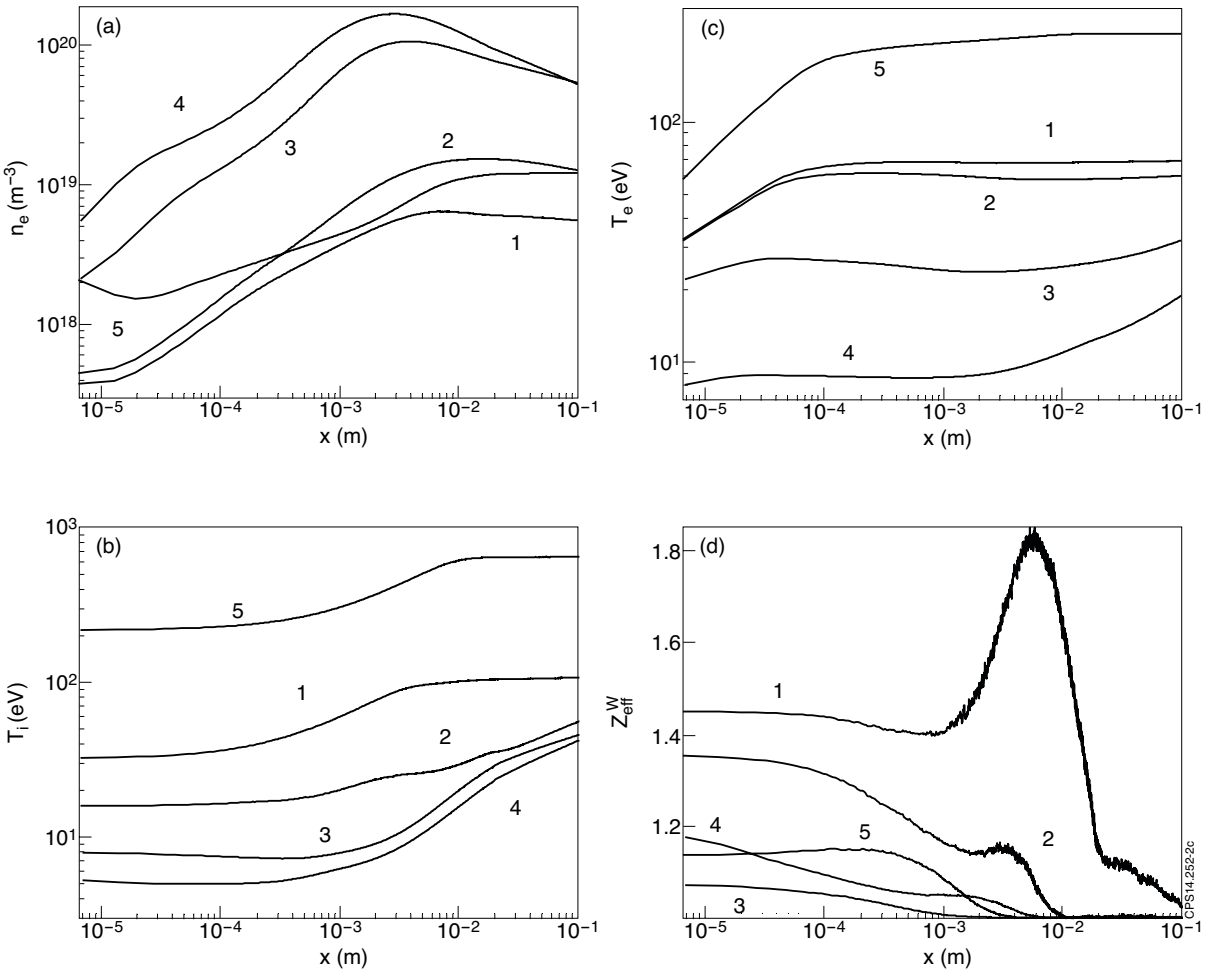

Figure 2: Plasma profiles in the inner divertor plasma. Numbers on the plots correspond to the cases from the table 1.

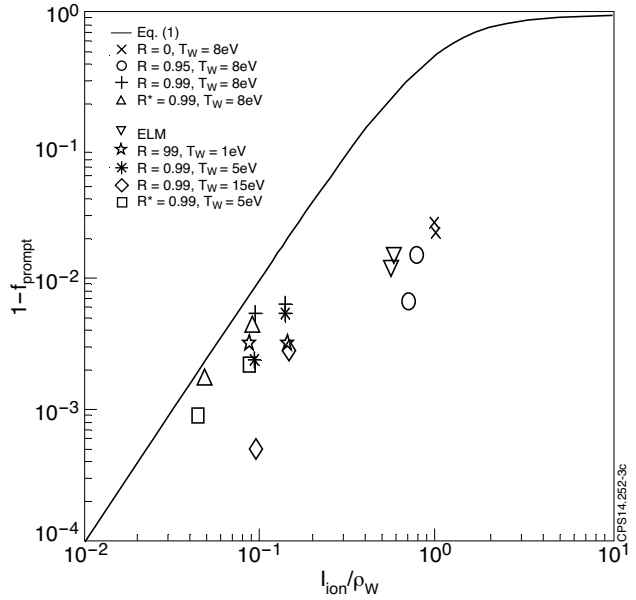

Figure 3: Prompt re-deposition coefficient from Eq. (1) and from PIC simulations. "" denotes the cases 4 and 9.*

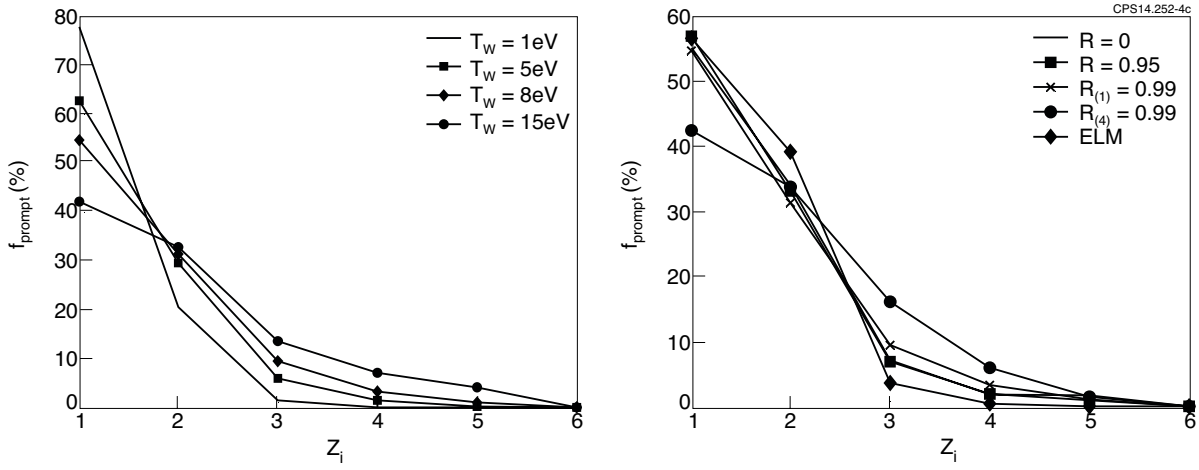

Figure 4: Distribution of the re-deposited W ion flux over ionization states. a) Dependence on the initial W atom temperature; b) dependence on plasma parameters.

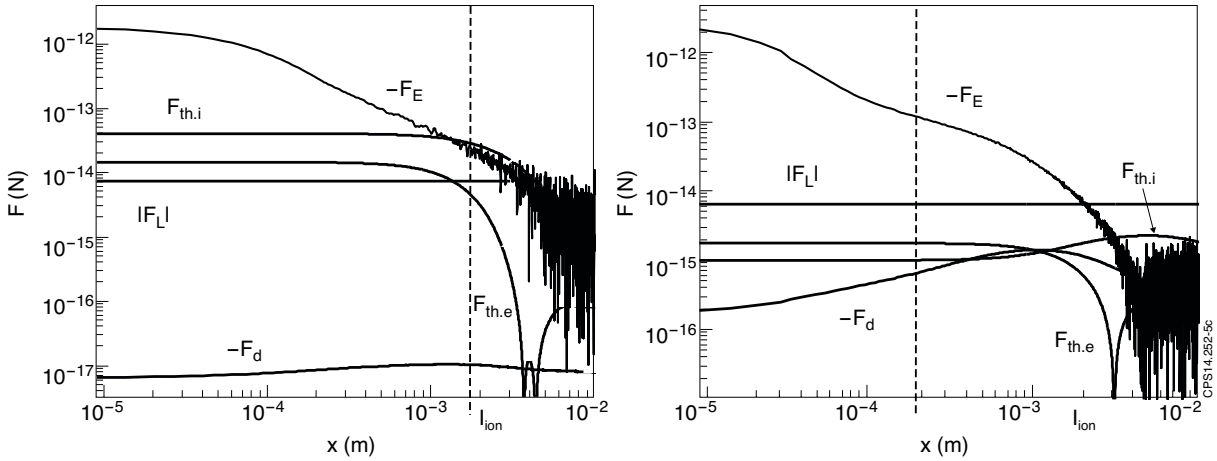

Figure 5: Forces acting on singly ionized W ion in the magnetic sheath. a) and b) correspond to the low and high collisional cases, 1 and 3, respectively.

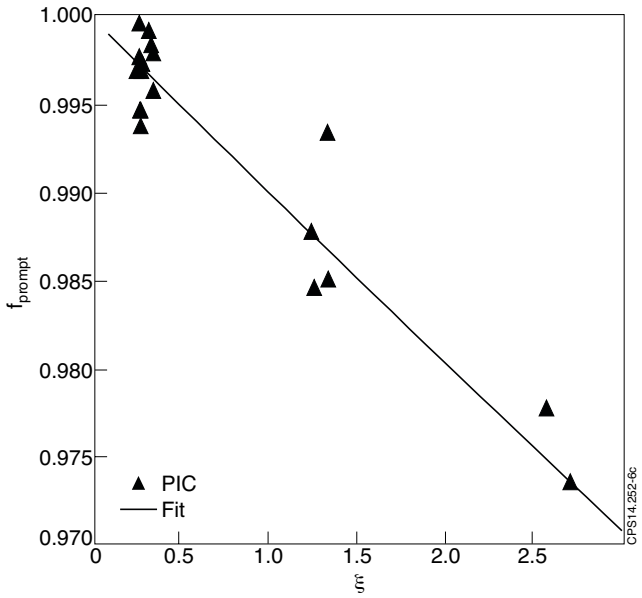

Figure 6: Prompt re-deposition coefficient from PIC simulations and the corresponding fit function (3) (with α = 0.01) vs $\xi = \frac{l_{ion}}{\rho_i}\frac{T_i}{T_e}$.

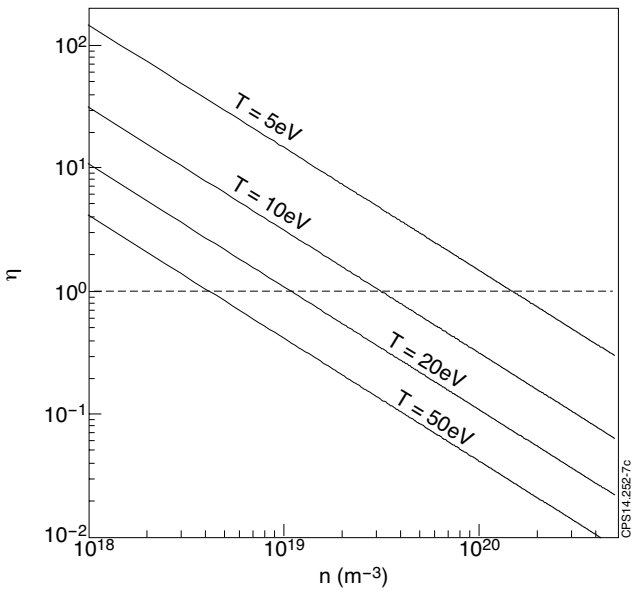

Figure 7: $\eta = l_{ion} / 5\rho_i$ *as a function of plasma density and temperature for ITER. Following assumptions are made: B = 5 T,* $T_e = T_i = T$, T_W = 10eV.